

Ozone and temperature changes in the stratosphere following the eruption of Mount Pinatubo

William J. Randel and Fei Wu

National Center for Atmospheric Research, Boulder, Colorado

J. M. Russell III

NASA Langley Research Center, Hampton, Virginia

J. W. Waters and L. Froidevaux

Jet Propulsion Laboratory, California Institute of Technology, Pasadena, California

Abstract. Global variations in stratospheric ozone and lower stratospheric temperature are documented for the period 1991–1994, following the eruption of Mount Pinatubo in June 1991. Column ozone measurements are from the total ozone mapping spectrometer instruments on the Nimbus 7 and Meteor 3 satellites, together with solar backscattered ultraviolet data from NOAA 11; these satellite ozone data are validated by comparisons with ground-based Dobson spectrophotometer measurements. Ozone profile data from the halogen occultation experiment and microwave limb sounder instruments on the upper atmosphere research satellite are also analyzed. Satellite temperature data are from the microwave sounding unit channel 4, representing a mean of the 150- to 50-mbar layer. The ozone observations show substantial decreases in column ozone (of order 5–10%) over large regions of the globe; largest losses are observed in northern hemisphere middle-high latitudes during winter–spring of each year (largest in 1992–1993), over southern hemisphere high latitudes in spring 1993, and episodically over the tropics during 1991–1993. Temperatures are anomalously warm (by order 1 K) over 30°N–S for 1 to 2 years following the eruption. Significant cold anomalies are also observed over the northern hemisphere polar cap during summer 1993, a result probably related to the decreased ozone levels throughout 1993.

1. Introduction

The eruption of Mount Pinatubo in June 1991 resulted in the formation of a dense cloud of sulfuric acid aerosol in the stratosphere. Although confined to the tropics for several months following the eruption, this aerosol cloud spread to extratropics of both hemispheres by the end of 1991 [Bluth et al., 1992; McCormick and Viega, 1992; Trepte et al., 1993]. Subsequent to this dispersal, record low global ozone values were reported in 1992 and 1993 from satellite data [Gleason et al., 1993; Planet et al., 1994; Herman and Larko, 1994] and from ground-based measurements [Bojkov et al., 1993; Kerr et al., 1993; Hofmann et al., 1994a; Komhyr et al., 1994]. Anomalously warm temperatures were also observed in the lower stratosphere during this time [Labitzke and McCormick, 1992; Angell, 1993; Spencer and Christy, 1993], similar to warmings observed after previous volcanic eruptions. In this paper we present a comprehensive view of the ozone and temperature anomalies observed during the 3 years following this eruption, based on satellite observations. We use column ozone data from the total ozone mapping spectrometer (TOMS) instruments onboard the Nimbus 7 and Meteor 3 satellites, together with solar backscattered ultraviolet

(SBUV/2) data from NOAA 11, and find consistent agreement between these independent measurements (although comparisons suggest omitting SBUV/2 data for measurements made at high solar zenith angles). We also compare these satellite data with ground-based Dobson spectrophotometer column ozone measurements and find good agreement; this validates the satellite measurements and gives global perspective to the station observations. We furthermore use the long record of satellite data (back to 1979) to statistically fit and remove variations (of order 2–4%) associated with the stratospheric quasi-biennial oscillation (QBO) and hence further isolate the volcanic associated anomalies. We also analyze ozone profile data from the halogen occultation experiment (HALOE) and microwave limb sounder (MLS) instruments on the upper atmosphere research satellite (UARS) satellite, which was launched in September 1991. Because UARS data are not available prior to Pinatubo, we compare the profile data between the years 1991–1994, using the TOMS and SBUV/2 data to select locations and time periods of near normal versus anomalously low column ozone.

The results presented here show local ozone depletions of order 5–10% during 1991–1994, which vary strongly in space and time. Large depletions are found over northern hemisphere (NH) middle-high latitudes during each winter–spring (persisting well into summer), with largest aerial extent and persistence during 1992–1993. These depletions are likely linked to heterogeneous chemical processes associated with the volcanic aerosol [Hofmann and Solomon, 1989; Brasseur and Granier, 1992;

Copyright 1995 by the American Geophysical Union.

Paper number 95JD01001.
0148-0227/95/95JD-01001 \$05.00

Hofmann *et al.*, 1994a; Rodriguez *et al.*, 1994; Tie *et al.*, 1994; Kinnison *et al.*, 1994]. Our results also highlight the record depth and aerial extent of the Antarctic ozone hole in 1993 (discussed by Hofmann *et al.* [1994b] and Herman *et al.* [1995]) and also show episodic ozone losses in the tropics over 1991-1993. Temperature anomalies show a significant warming of the tropical stratosphere (over approximately 30°N-S) by 0.5-1.5 K (over the 150- to 50-mbar layer sampled by microwave sounding unit (MSU)), which persists for 1 to 2 years following the eruption. We also find significant cooling of the NH polar lower stratosphere during summer 1993, which is notable because "natural" interannual variability is very small in summer. This cooling is likely related to the depleted ozone levels observed over the NH throughout 1993.

2. Data and Analyses

TOMS data analyzed here are gridded Version 6 retrievals from the Nimbus 7 satellite covering January 1987-April 1993, combined with data from the Meteor 3 satellite over September 1991-December 1994. All results here are based on monthly mean data. Comparisons between data from these two instruments for the overlap period (September 1991-April 1993) showed relatively small differences (typically 1-2% [see Gleason *et al.*, 1993, Figure 5]). These data sets are combined by simply appending Meteor 3 data to the Nimbus 7 record after April 1993; these data are referred to hereinafter simply as TOMS data. As a note, the orbit of the Meteor 3 satellite has drifted with time, and the TOMS Meteor 3 data are considered less reliable when the equator crossing time of the satellite is greater than 3 hours on either side of noon/midnight (when the spacecraft is flying near the terminator). We have included all the Meteor 3 data in the figures here but include marks on the figures denoting times of these less reliable data.

SBUV/2 total ozone data are Version 6 retrievals from the NOAA 11 satellite, covering January 1989-April 1994 (data for March 1991 are unavailable). These orbital data have been mapped using a Kalman filter technique, and the daily data are averaged to produce monthly means. Comparison of the post-Pinatubo SBUV/2 and Nimbus 7 TOMS data showed an offset of approximately 3% over all latitudes, plus substantially larger differences (in excess of 10%) at high winter latitudes. The 3% bias is related to prelaunch TOMS wavelength calibration effects (J. Gleason, personal communication, 1994), whereas the larger high-latitude differences are suggestive of solar zenith angle effects on the SBUV/2 measurements. Bhartia *et al.* [1993] discuss the effect of enhanced aerosol loading on SBUV/2 total ozone retrievals, showing that large underestimates may occur for measurements made at high solar zenith angle (high latitudes for a Sun-synchronous orbit). Figure 1 shows the (SBUV/2-TOMS) differences plotted versus solar zenith angle of the SBUV/2 measurements, clearly showing an increase in the differences for solar zenith angles greater than ~80° (this effect is reduced in TOMS data because it scans horizontally across the orbit track, as opposed to the nadir viewing SBUV/2 measurements [see Bhartia *et al.*, 1993]). Based on these comparisons, we do not use SBUV/2 data for solar zenith angles greater than 80°. In order to extend the SBUV/2 record back to 1987, we have used SBUV column ozone measurements from the Nimbus 7 satellite; these show small differences from SBUV/2 for the overlap period January 1989 - June 1990.

The ozone and temperature anomalies discussed here are calculated as differences from a seasonally varying pre-Pinatubo

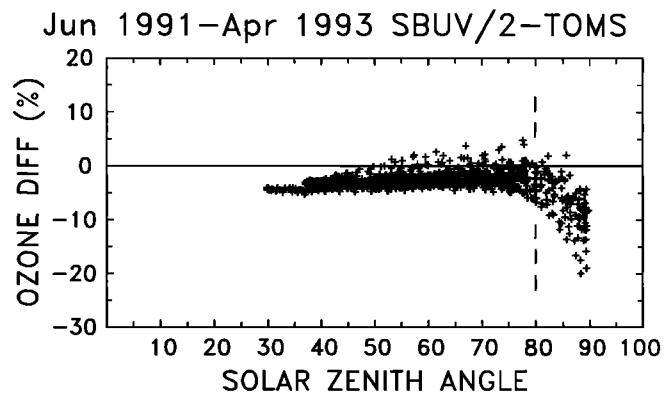


Figure 1. Percentage differences between SBUV/2 and TOMS column ozone measurements for July 1991-April 1993, plotted versus the solar zenith angle of the SBUV/2 measurements. Each point represents a monthly mean at a particular latitude. Note the large differences for solar zenith angles greater than 80°.

average calculated over the four years 1987-1990. These differences are used for simplicity of calculation and interpretation, and a 4-year average is taken to minimize quasi-biennial oscillation (QBO) effects. Furthermore, both TOMS and SBUV/2 column ozone data show systematic biases with ground-based measurements that are strongly seasonally dependent (and different between TOMS and SBUV/2 [see *World Meteorological Organization* (WMO), 1995, Chapter 1]); the differences calculated here will minimize these seasonal biases. Assuming linear ozone decreases between this 1987-1990 reference and the 1991-1994 time period analyzed here equal to those reported by Stolarski *et al.* [1991], differences of order 2% over NH midlatitudes and 2-4% over southern hemisphere (SH) middle to high latitudes might be expected (much less in the tropics). We thus focus discussion here on ozone anomalies (differences) larger than 4%.

In order to validate the satellite-derived ozone changes shown here, we have made comparisons with ground-based Dobson spectrophotometer column ozone measurements. We obtained monthly mean Dobson measurements for the eight stations discussed by Komhyr *et al.* [1994] and for the five stations with long-term records analyzed by Kerr *et al.* [1993]. As with the satellite data, we calculate Dobson ozone differences over 1991-1994 compared to the 4-year average 1987-1990. In general the satellite and ground-based column ozone data show good agreement (we show a subset of the comparisons below), lending confidence to the global patterns revealed in the satellite analyses.

The HALOE ozone profile measurements analyzed here are discussed by Russell *et al.* [1993]. HALOE is a solar occultation instrument, providing measurements over a narrow latitude range on a given day; this latitudinal sampling shifts in time, so that much of the globe is sampled over approximately 1 month. The vertical resolution of the HALOE data is near 2 km. The MLS is a passive microwave sounding instrument whose characteristics are discussed by Froidevaux *et al.* [1994], who also presents analyses of zonal mean ozone variations over the time period analyzed here. MLS ozone data are available over much of the globe on a daily basis; the data used here have been synoptically mapped using a Kalman filter algorithm, and we then calculate monthly means. The MLS data have a vertical resolution of approximately 3 km, but only data at every other archived pressure level are actual retrieved values (at 100., 46., 22., 10., 4.6, 2.2, 1. and 0.46 mbar); data between these levels are

interpolated values. We have smoothed both the HALOE and MLS data used here slightly in the vertical.

Because data from HALOE and MLS are not available prior to September 1991, we cannot directly compare pre- versus post-Pinatubo measurements as with the TOMS and SBUV/2 data. Rather, we compare monthly means at selected locations between the individual years over 1991-1994, using the TOMS and SBUV/2 data to select periods of near-normal versus anomalously low column ozone. We find that the column ozone differences between these years calculated with HALOE and MLS data agree well with those observed in TOMS and SBUV/2 measurements, and the profile data then illustrate where (in altitude) the column anomalies originate.

The MSU channel 4 temperature data analyzed here provide a measure of the weighted mean temperature in the 150- to 50-mbar layer (approximately 13-22 km), with maximum contribution from altitudes near 17 km [see *Spencer and Christy, 1993*]. It is important to note this layer lies entirely in the lower stratosphere over middle to high latitudes, whereas in the tropics it spans the upper troposphere and lower stratosphere (the weighting function maximum is near the tropical tropopause). A continuous global record is provided by the series of MSU instruments on National Oceanic and Atmospheric Administration (NOAA) operational satellites, and intercalibration provides an extremely stable time series (precision of individual monthly and zonal means, as analyzed here, is of order 0.01-0.03 K [Spencer and Christy, 1993]). The data analyzed here have been reprocessed to remove a slow negative drift (after 1991) attributable to the precessing orbit of the NOAA 11 satellite (J. Christy, personal communication, 1994).

3. Ozone Observations

Figure 2a shows the latitude-time evolution of zonal mean column ozone anomalies over 1991-1994 from TOMS data (anomalies defined as differences from the 1987-1990 average), and Figure 2b shows the equivalent result from SBUV/2 data (until April 1994). Note that the SBUV/2 data have substantially more missing observations, due to exclusion of data with high solar zenith angle (see section 2), and also the drift in time of the NOAA 11 satellite orbit. Over the regions sampled by both TOMS and SBUV/2, the anomalies show very similar patterns and magnitudes, enhancing confidence in each individual satellite's measurements. To further confirm these satellite data, Figure 3 shows comparisons of the monthly anomalies from ground-based Dobson measurements with results from Nimbus 7 TOMS, Meteor 3 TOMS, and SBUV/2 satellite measurements (at the station locations); results are shown for six stations widely spaced in latitude (Resolute, 75°N; Edmonton, 54°N; Caribou, 47°N; Boulder, 40°N; Mauna Loa, 20°N; Samoa, 14°S). Figure 4 furthermore shows scatter diagrams of satellite versus Dobson anomalies for all 13 Dobson locations, with separate plots for TOMS Nimbus 7, TOMS Meteor 3, and SBUV/2 data (the latter separated for solar zenith angles less than and greater than 80°). The comparisons in Figures 3 and 4 show overall reasonable agreement between the satellite and Dobson data (and between the individual satellite measurements), lending confidence to the large-scale patterns shown in Figure 2. Note also that the high solar zenith angle SBUV/2 anomalies exhibit a negative bias with respect to the Dobson data in Figure 4, consistent with the SBUV/2-TOMS differences shown in Figure 1.

Analysis of TOMS data has revealed a significant component of interannual variability associated with the quasi-biennial

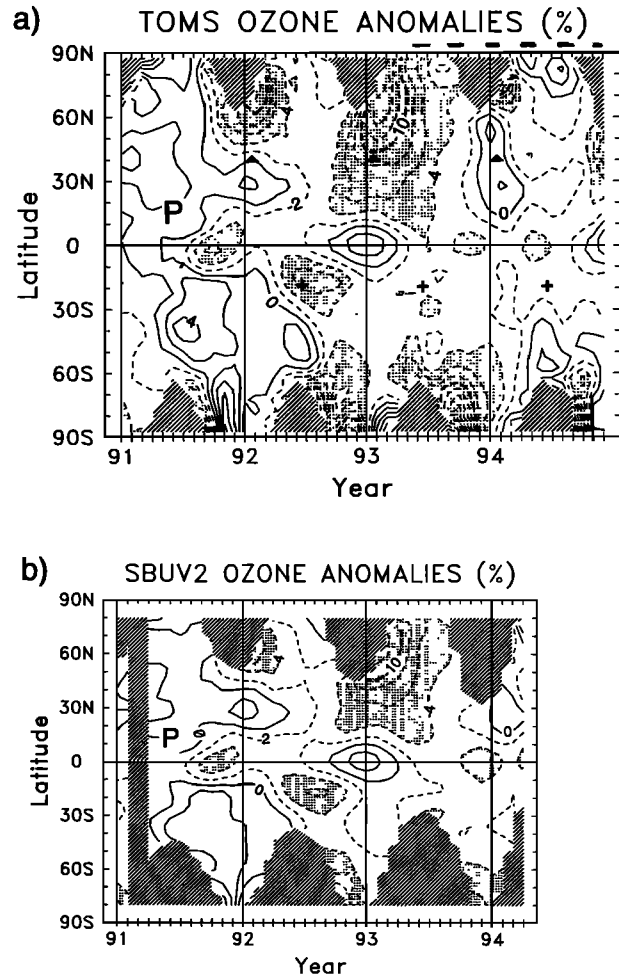


Figure 2. Latitude-time diagrams of column ozone anomalies during 1991-1994 measured by (a) TOMS and (b) SBUV/2. Anomalies are calculated as percentage differences from the 1987-1990 seasonally varying mean and smoothed in time with a running 1-2-1 filter. Hatched regions denote that data are unavailable (due to polar night for TOMS data, and for solar zenith angles $> 80^\circ$ for SBUV/2 data). Solid bars in the upper right hand corner of Figure 2a denote time periods when TOMS Meteor 3 data are considered less reliable (see text). P marks the eruption of Mount Pinatubo. Triangles and plus signs in Figure 2a denote locations of the ozone profile comparisons in Figures 8 and 11, respectively.

oscillation (QBO) of the tropical lower stratosphere; local zonal mean variations of $\pm 2-4\%$ are evident, extending well outside of the tropics [Bowman, 1989; Shiotani, 1992; Randel and Cobb, 1994; Yang and Tung, 1994]. We model and remove this QBO signal here using seasonally varying regression analysis as by Stolarski *et al.* [1991] and Randel and Cobb [1994]. We use here an improved reference time series for these QBO ozone variations, based on a linear combination of the equatorial zonal winds over 70-10 mbar, rather than winds at any particular level (motivated by the study of Wallace *et al.* [1993]). Our reference time series uses a weighted average of the zonal winds over 70-10 mbar with the following weights: 10 mbar (0.24), 15 mbar (0.51), 20 mbar (0.60), 30 mbar (0.50), 40 mbar (0.26), 50 mbar (0.04), and 70 mbar (-0.09). These were derived by linear regression between the observed (deseasonalized) equatorial ozone

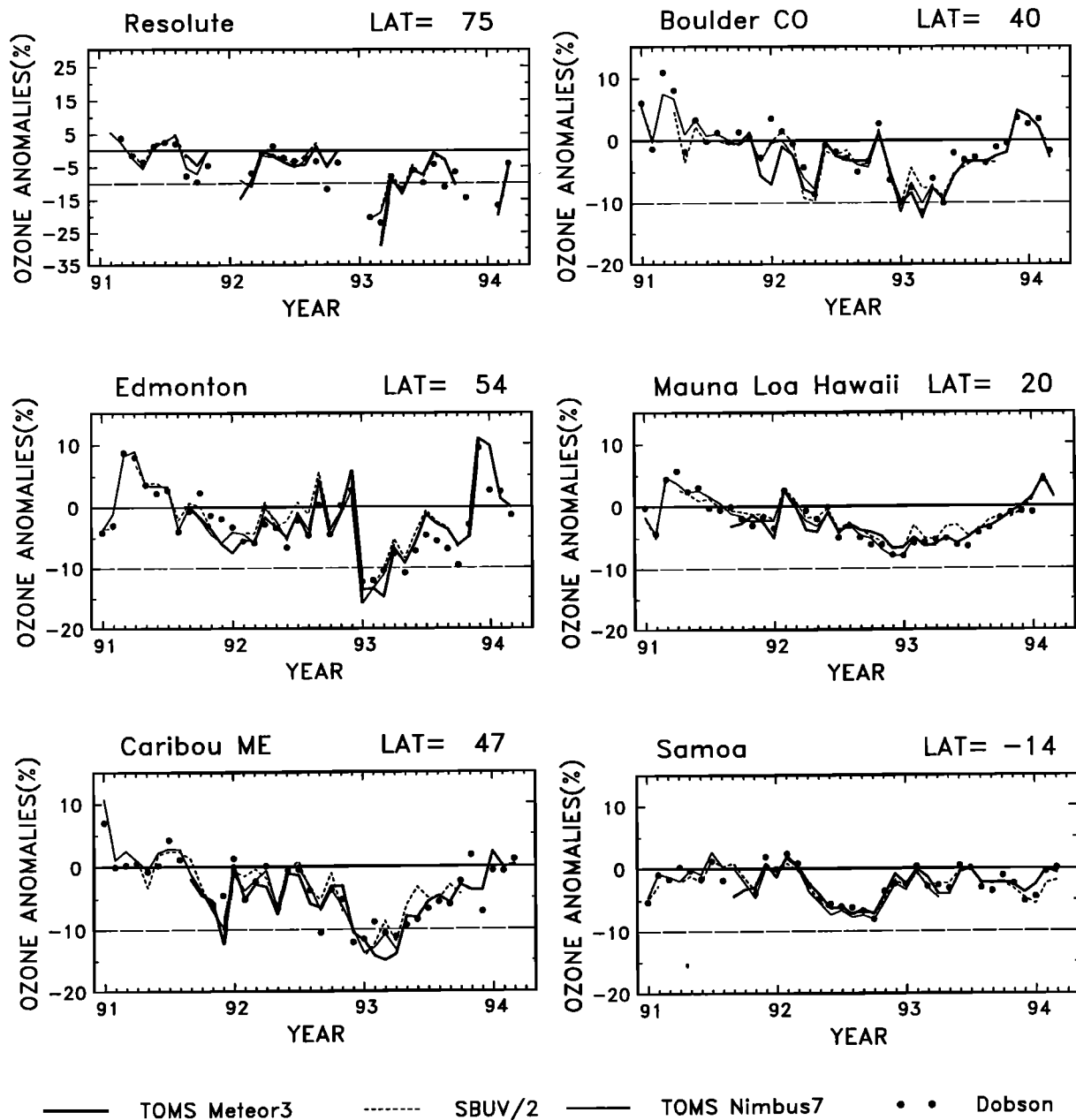


Figure 3. Monthly mean column ozone anomalies over 1991-1994 measured by Dobson spectrophotometer at several locations (noted above each panel), compared to satellite observations at these positions. Anomalies are calculated as percentage differences from the 1987-1990 mean.

anomalies and the zonal winds at the above pressure levels, calculated for data over 1979-1991 (before Pinatubo). Figure 5 shows the resulting QBO reference time series (dependent solely on the zonal winds), together with the observed equatorial ozone anomalies. The correlation between these time series is 0.92 during 1979-1991, compared with 0.65 using a 30 mbar zonal wind reference time series (the best individual level).

Extratropical ozone anomalies associated with the QBO are out of phase with the tropical patterns, and strongly seasonally dependent (occurring only during winter-spring of the respective hemispheres [see Chandra and Stolarski, 1991; Randel and Cobb, 1994; Yang and Tung, 1994]). This seasonal dependence in extratropics is the reason why it is important to use a regression analysis that is seasonally varying in modeling these variations.

Figure 6 shows the observed deseasonalized ozone anomalies at 30°N and 30°S over the entire TOMS record (1979-1994), together with the regression-derived QBO fits at these locations. The QBO fits are derived from the 1979-1991 (pre-Pinatubo) period and extended into 1994 using updated values of the QBO winds. These statistically derived QBO variations over 1991-1994 are then subtracted from the "total" anomalies shown above (Figure 2).

Figure 7 shows the TOMS ozone anomalies (from Figure 2a) with the statistical QBO signal removed, and this is our best estimate of the "true" anomalies over this time period (attributable to Pinatubo plus any other "natural" or forced variations). Zerefos *et al.* [1994] show similar results for the period 1991-early 1993. Ozone variations associated with solar

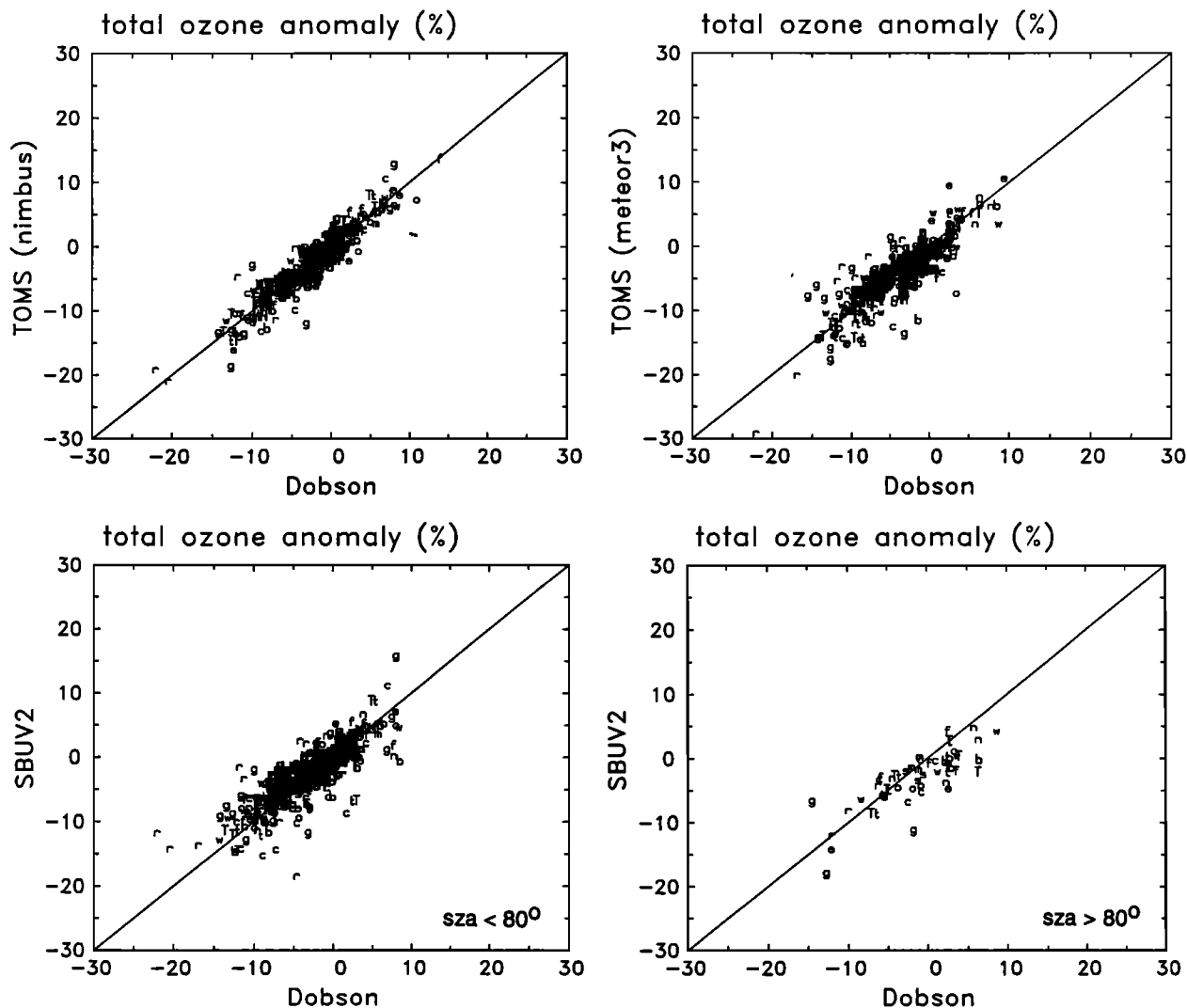


Figure 4. Scatter diagrams comparing satellite versus Dobson column ozone anomalies during 1991-1994, based on data at 13 Dobson stations (see text). Results are shown for (top left) TOMS Nimbus 7, (top right) TOMS Meteor 3, and (bottom panels) SBUV/2 data. The SBUV/2 comparisons are separated for solar zenith angle (sza) < 80° (bottom left) and ≥ 80° (bottom right).

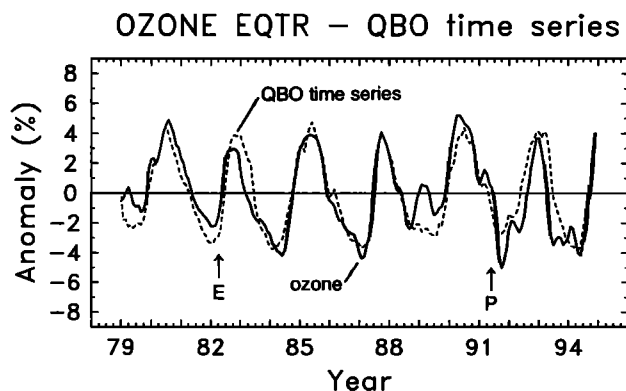


Figure 5. Solid line shows deseasonalized TOMS column ozone anomalies (in percent) over the equator during 1979-1994. Dashed line is the QBO reference time series derived from a linear combination of the equatorial zonal winds over 70-10 mbar (see text). The variance of the dashed line has been set equal to that of the solid line. E and P denote El Chichon and Pinatubo, respectively.

cycle forcing and El Nino-Southern Oscillation climate anomalies have also been observed in TOMS data [Hood and McCormack, 1992; Shiotani, 1992; Randel and Cobb, 1994]. Projection of the TOMS anomalies during 1979-1991 onto solar proxy time series shows solar maximum-solar minimum variations near 2% [Stolarski et al., 1991; Hood and McCormack, 1992; Randel and Cobb, 1994]. However, this fit is possibly confused by the declining solar cycle during 1982-1983 overlapping effects of the El Chichon volcanic eruption in April 1982, and we choose not to attempt removal of the solar cycle effect based on the relatively short record of TOMS data. (We note that the solar signal in satellite ozone data will be further confused by decline of the solar cycle during 1992-1993 coinciding with Pinatubo effects.) ENSO ozone variations are mainly longitudinally localized [Shiotani, 1992; Randel and Cobb, 1994; Zerefos et al., 1994]; zonal mean variations (as studied here) are of order 1%, and we do not attempt their removal here either. "Natural" variations of column ozone (those attributable to normal month-to-month meteorological variability inherent to the atmosphere) are of order 2% in midlatitudes, and 1% in the tropics (these are standard

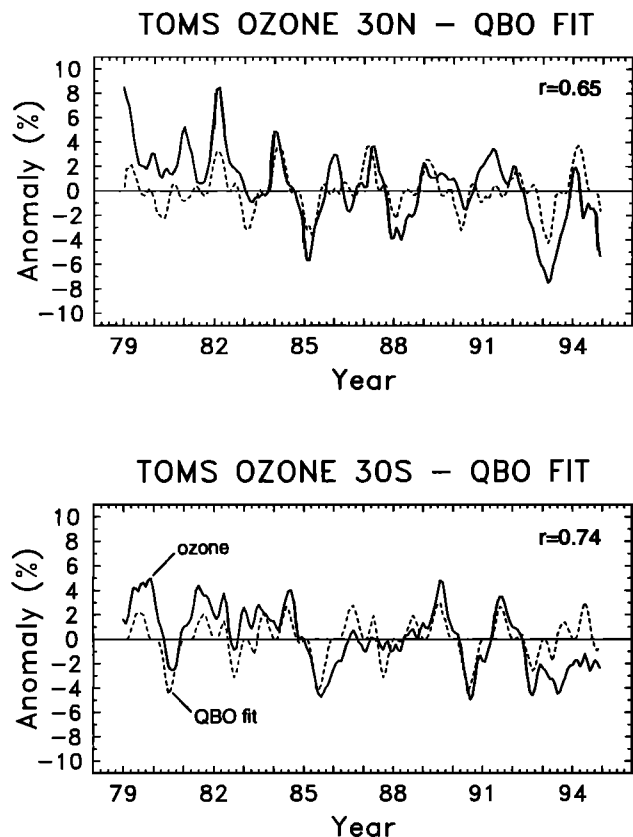


Figure 6. Solid lines are deseasonalized TOMS column ozone anomalies at (top) 30°N and (bottom) 30°S over 1979-1994. Dashed lines are the statistical QBO fits to these time series using seasonally varying regression.

deviations of monthly mean residuals, from *Randel and Cobb*, 1994, their Figure 15). The ozone losses during 1991-1994 discussed below are of order 5-10%, substantially larger than such natural variability.

There are several areas of large ozone decreases seen in Figure 7, and these are discussed in turn here. Ozone losses of order 4% are seen in the tropics for several months following the eruption (September-November 1991). This initial tropical ozone depletion has been discussed by *Chandra* [1993] and *Schoeberl et al.* [1993]; their estimates of the magnitude (~6%) did not take into account the effect of the QBO (note this time period in Figure 5). This initial ozone loss is likely related to radiative heating of the Pinatubo aerosol, followed by upward vertical velocities and decreased column ozone due to transport [*Brasseur and Granier*, 1992; *Kinne et al.*, 1992; *Pitari and Rizzi*, 1993; *Tie et al.*, 1994; *Young et al.*, 1994]. Largest temperature perturbations were observed in the tropical lower stratosphere at this time (*Labitzke and McCormick* [1992], show September-October 1991 zonal mean increases near 2.5°C over 30-50 mbar; see also the MSU data below in Figure 13), consistent with this explanation. *Tie et al.* [1994] furthermore suggest that changes in ozone photolysis rates (associated with light backscattered by the aerosol cloud) are important for ozone changes at this time.

Large ozone decreases are seen during NH winters 1991-1992 and 1992-1993; these have been reported from satellite data of *Gleason et al.* [1993], *Planet et al.* [1994], and *Herman and Larko* [1994], and also from ground-based measurements [*Bojkov et al.*, 1993; *Kerr et al.*, 1993; *Hofmann et al.*, 1994a; *Komhyr et*

al., 1994]. Figure 7 shows zonal mean decreases during 1991-1992 somewhat in excess of 10% (during February-March 1992, polewards of 60°N). The absolute magnitude of maximum loss is similar for 1992-1993 (10-12%), but the aerial extent of the depleted region is much larger than for the 1991-1992 winter (in particular reaching to much lower latitudes). Losses occur early in winter during both years (during November-December), well before the occurrence of polar stratospheric cloud (PSC) threshold temperatures at high latitudes [*WMO*, 1995, Chapter 3]. Decreased ozone levels above 4% persist into NH summer for both years (into June 1992 and August-September 1993), and during May-June 1993 the -4% contour reaches the equator (this is the period of largest global mean depletion; see Figure 15 below). Ozone losses of order 10% are seen over NH high latitudes in February-March 1994 (see also data from *Resolute* in Figure 3), and losses somewhat larger than 4% are found over NH midlatitudes during April-June 1994 (although midlatitude values were near or above normal in midwinter).

Figure 8 shows the vertical profiles of ozone mixing ratio over 35°-45°N during January 1992, 1993, and 1994 from HALOE, and during January-February 1992, 1993, and 1994 from MLS. This location and time is chosen based on the data in Figure 2, which show relatively small column depletions in 1992 and 1994, but losses near 10% in 1993. Figure 8 clearly shows lowered ozone amounts below 35 km in 1993 as compared to the other years in both HALOE and MLS data. Integration of the column amounts above 100 mbar give 1992, 1993, and 1994 values of 262, 235, and 268 (280, 259, 288) Dobson unit (DU) from HALOE (MLS) data, respectively. Column amounts were thus 10-12% lower in 1993 than in 1992 or 1994, in agreement with the TOMS and SBUV/2 column differences. Figure 9 shows the percent differences between 1993 and the other years, showing local ozone profile depletions of order 10% over 25-35 km, and larger percentage losses (20-30%) near 17-20 km. The majority of the column difference originates in the 19- to 27-km layer. *Hofmann et al.* [1994a] report 20-30% ozone depletions near 20 km in 1993, based on ozonesonde data comparisons with pre-Pinatubo data. They also find an increase in ozone above 25 km between the pre- and post-Pinatubo periods that is not seen in the satellite data comparisons between 1992 and 1994.

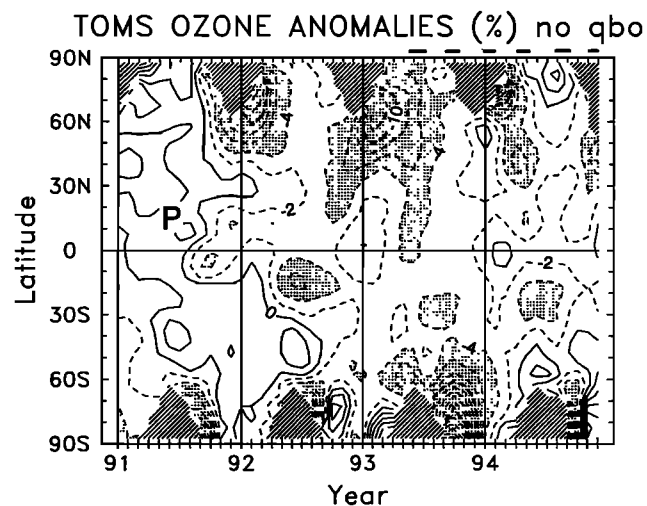


Figure 7. Latitude-time diagram of column ozone anomalies over 1991-1994 measured by TOMS (as in Figure 2a), but with the effect of the QBO removed by statistical regression (see text).

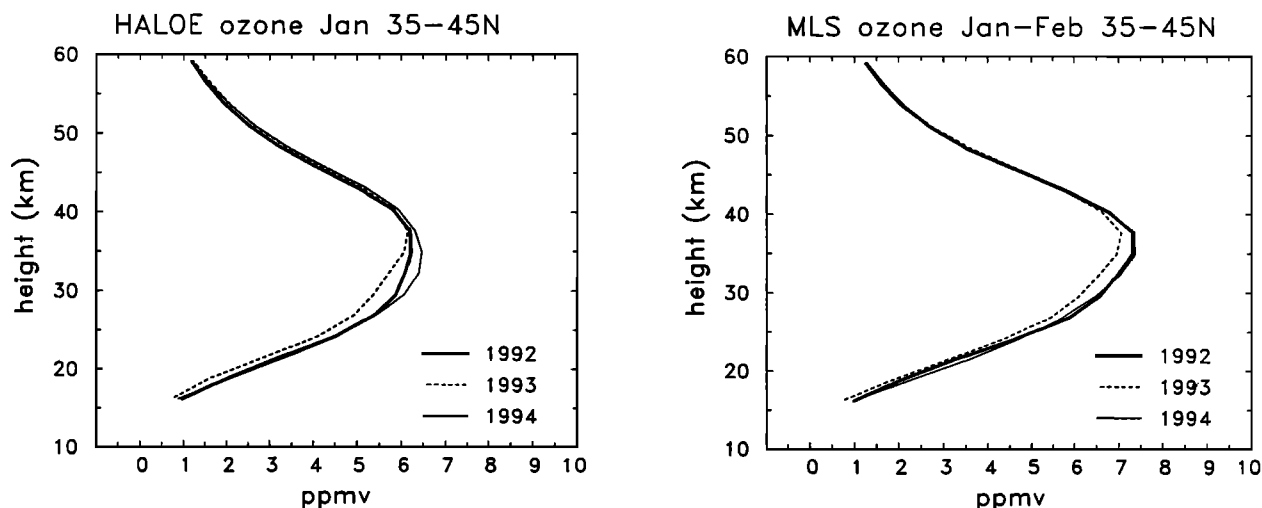


Figure 8. Vertical profiles of ozone mixing ratio (parts per million by volume (ppmv)) over 35°-45°N based on (left) HALOE data and (right) MLS data during January-February 1992, 1993, and 1994.

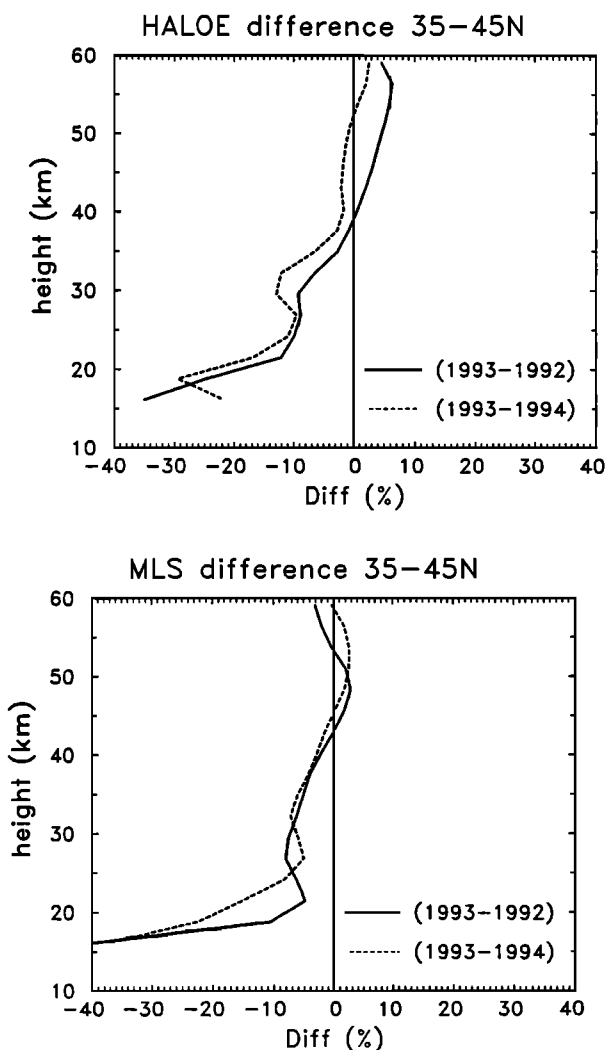


Figure 9. Ozone profile differences over 35°-45°N during northern hemisphere winters of 1992, 1993, and 1994, based on (left) HALOE and (right) MLS data from Figure 8.

Ozone losses in excess of 6% are seen in the SH subtropics (10°-25°S) during May-November 1992 in Figure 7 (and in SBUV/2 data in Figure 2b), and also clearly in the Samoa Dobson data in Figure 3. These subtropical losses were noted by *Gleason et al.* [1993] and *Grant et al.* [1994], but have received little attention since then. Figure 10 shows time series of column ozone anomalies over 10°-20°S for each year of the TOMS record (1979-1994), demonstrating that the 1992 departures were more than twice as large as anomalies during any recent year. These losses in the SH subtropics a year after the eruption are clearly distinct from the tropical losses due to radiative-induced lifting effects (over September-November 1991) discussed above, and their cause is yet to be determined.

Figures 11 and 12 show ozone profile comparisons and differences over 10°-25° S during July 1992, 1993, and 1994 from HALOE, and June 1992, 1993, and 1994 from MLS. This latitude band and time period are chosen to study the large depletions seen in 1992 (but not 1993 or 1994) in TOMS and SBUV/2 data (Figure 2). Calculated column ozone from these profiles (above 100 mbar) for 1992, 1993, and 1994 are 218, 228,

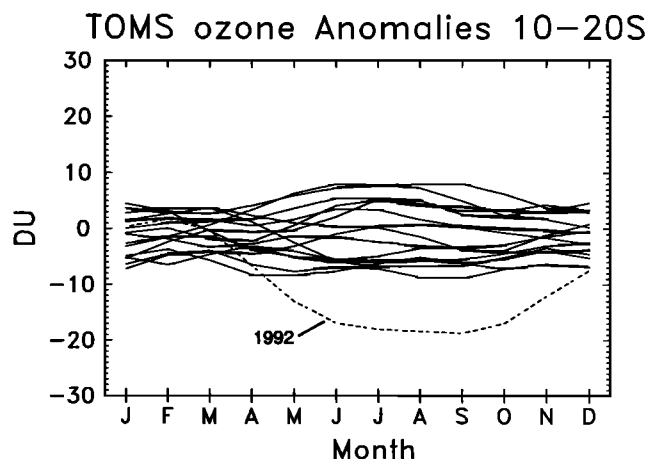


Figure 10. Time series of monthly mean TOMS column ozone over 10°-20°S, for each individual year during 1979-1994. The dashed line indicates data for 1992.

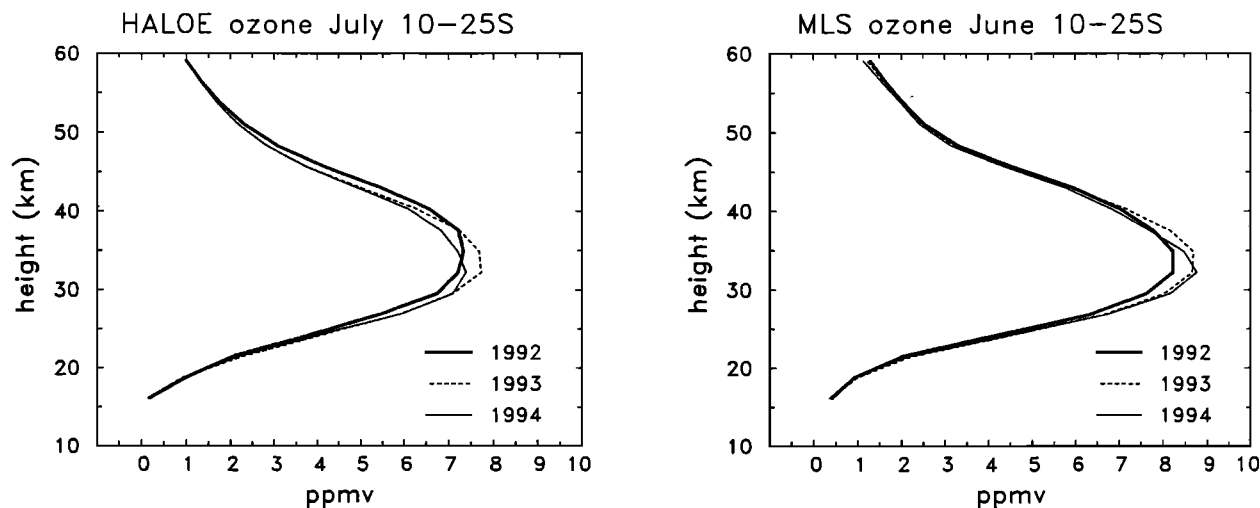


Figure 11. Vertical profiles of ozone mixing ratio (parts per million by volume (ppmv)) over 10° - 25° S for (left) HALOE data and (right) MLS data during June-July 1992, 1993, and 1994.

and 224 (240, 251, and 250) DU from HALOE (MLS) data, respectively. These show approximately 5% lower values in 1992, similar to the measured column differences seen in Figure 2. The profile differences in Figure 12 show that ozone in 1992 is approximately 5-10% lower over 22-35 km, but the depleted region does not extend below 20 km (as did the midlatitude depletions in Figure 9). The majority of the column differences originate in the 22- to 30-km layer. These SH subtropical data also show concomitant ozone profile increases of 3-10% over 40-55 km, although these have little impact on the column.

A further region of large ozone depletion is seen in Figure 7 associated with the Antarctic ozone hole during the SH spring of 1993. *Herman et al.* [1995] show details of the 1993 ozone hole observations by Meteor 3 TOMS, and document good agreement with ground-based Dobson data. Ozone anomalies of order 10-20% are seen in Figure 7 over high latitudes during October-December 1993; the -4% isoline extends to 45° S and persists well into SH summer (February 1994). Record low ozone values over the south pole at this time were reported by *Hofmann et al.*

[1994b], and they attributed these to prolonged cold temperatures, Pinatubo aerosols, and increased chlorine levels over prior years. The persistence far into summer of these anomalies (and likewise those in the NH) is similar to transport-induced effects observed in a recent model simulation of the Antarctic ozone hole [*Mahlman et al.*, 1994]. We note that the depth and spatial extent (as measured by the 220 DU contour) of the ozone hole in 1994 was similar to that in 1993; however, Figure 7 shows that during 1993 regions of decreased ozone reached to much lower latitudes (well outside of the vortex).

4. Temperature Anomalies

Figure 13a shows the MSU temperature anomalies during 1991-1994, and Figure 13b shows the anomalies after statistical removal of the QBO signal (these latter being the focus of further discussion). Substantial variability is seen over high winter latitudes of both hemispheres (polewards of 50° N-S), related to the presence or absence of stratospheric warming events during

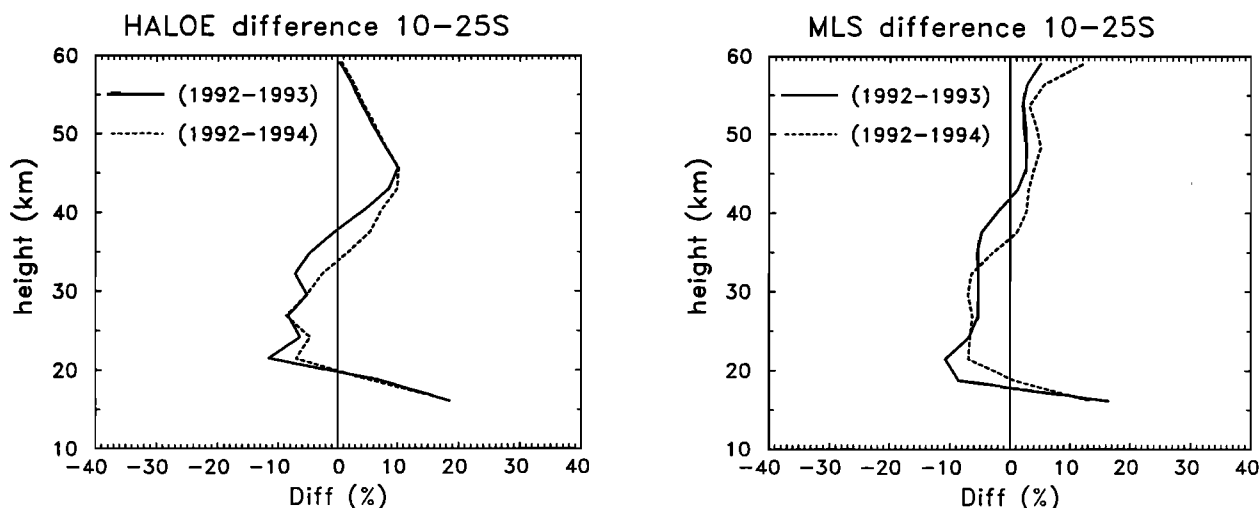


Figure 12. Ozone profile differences over 10° - 25° S during southern hemisphere winters of 1992, 1993, and 1994, based on (left) HALOE and (right) MLS data from Figure 11.

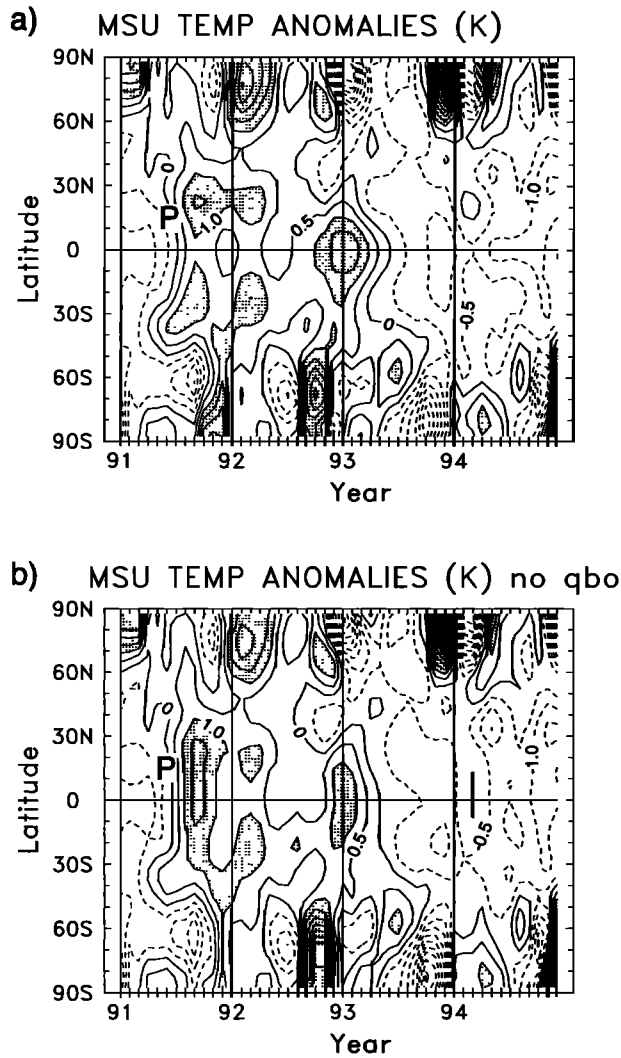


Figure 13. (a) Latitude-time variation of MSU temperature anomalies during 1991-1994, calculated as differences from the 1987-1990 mean. (b) Anomalies after statistical removal of QBO effects.

individual months. In contrast, warm anomalies are observed over the tropics from shortly after the eruption until early 1993. Anomalies of order 1-1.5 K are observed over approximately 40°N-S from August 1991 until April 1992, with a maximum during September-October 1991 over 10°S-30°N (the timing of this maximum agrees well with the tropical temperature increases reported by *Labitzke and McCormick* [1992], and with the localized tropical ozone depletion seen in Figure 7; see discussion above). Tropical warm anomalies of 0.5-1 K are observed over SH subtropics (10°-30°S) during the middle of 1992, and over 20°N-S during November 1992-April 1993. The warm anomalies end abruptly in early 1993, coincident with the phase change of the QBO (see Figure 5), and tropical temperatures have remained anomalously cold through the end of 1994.

Cold temperature anomalies of order 1 K are observed in NH polar regions during summer 1993 in Figure 13. These are remarkable because “natural” interannual temperature variability in the summer polar lower stratosphere is very small (standard deviation < 0.5 K), so that 1 K anomalies are significant. Figure 14 shows the MSU monthly mean anomalies over the polar cap for each year 1979-1994, illustrating both the low variability

during summer and the anomalously cold temperatures during summer 1993. Given the record low ozone values observed over high latitudes throughout 1993 (Figures 2 and 3), it is likely that ozone-related radiative effects contribute to these anomalous cold polar temperatures [e.g., *Ramaswamy et al.*, 1992].

5. Summary and Discussion

Column ozone anomalies over 1991-1994 seen in TOMS and SBUV/2 data agree well with each other and also compare well with anomalies calculated from ground-based measurements over a wide range of latitudes, lending confidence to the global anomaly patterns derived here. The long record of satellite data furthermore allows accurate isolation and removal of QBO effects, resulting in the ozone anomaly patterns shown in Figure 7, and the temperature anomalies in Figure 13b. The global integrals of these anomalies (over 65°N-S) are shown in Figure 15, including data from 1979-1994 for perspective. The ozone curve shows decreasing global values over approximately 1981-1984, near constant values from 1985-1990, and then strong depletions following Pinatubo. The temperature curve in Figure 15 clearly shows the warming episodes attributable to El Chichon and Pinatubo, which were approximately of similar magnitude and duration (as seen by MSU channel 4).

Although the global integral of column ozone decrease following Pinatubo looks monotonic for 1991-1993 in Figure 15, it is actually comprised of a series of episodic losses in the tropics and middle-high latitudes of both hemispheres (Figure 7). The initial tropical losses and the NH midlatitude depletions have been discussed in some detail (see references above), whereas the ozone loss in the SH subtropics during May-November 1992 has received little attention. We note that a weak warm temperature anomaly is observed in the lower stratosphere near this location and time (see Figure 13b). The combination of negative ozone anomaly and positive temperature anomaly is similar to that observed in the tropics shortly after the eruption (September-October 1991, discussed above), but opposite to the similarly signed ozone-temperature perturbations expected for both dynamically and radiatively driven coupling [see *Randel and Cobb*, 1994]. The cause of the (large) ozone losses at this time remain to be explained. There are also tropical ozone losses of order 2-4% throughout most of 1993; the largest global mean

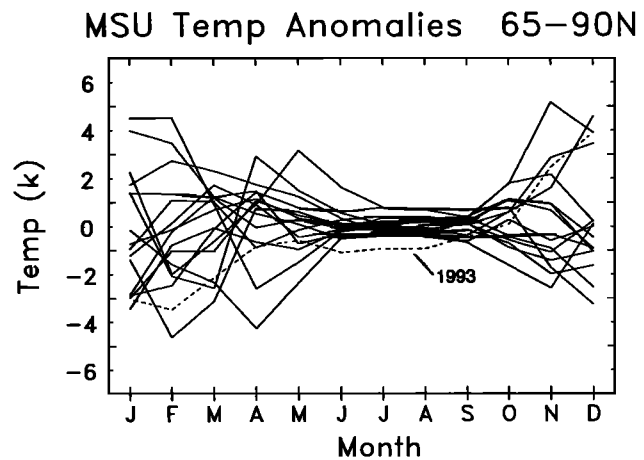


Figure 14. Time series of monthly mean MSU temperature anomalies over 65°-90°N for each individual year during 1979-1994. The dashed line indicates data for 1993.

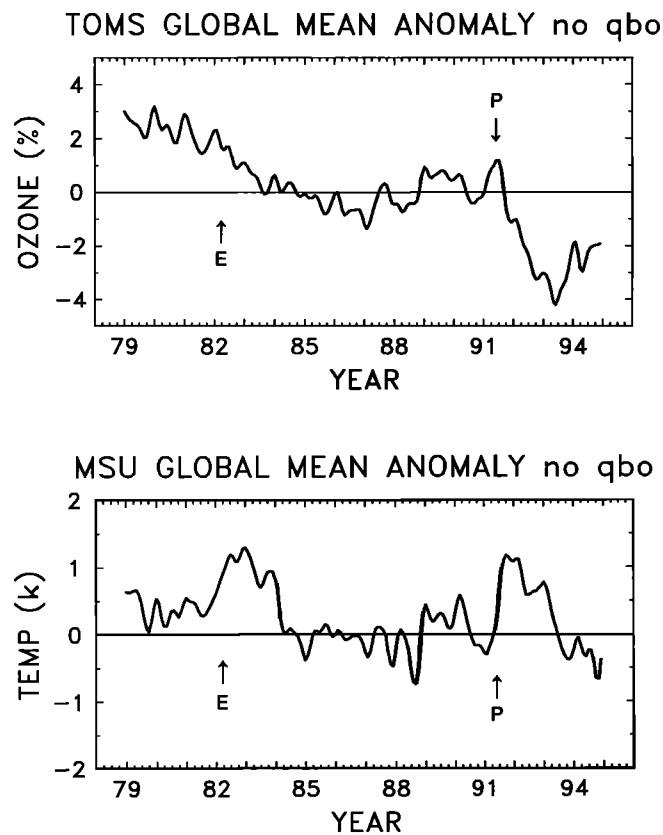


Figure 15. Globally integrated (65°N-S) and area weighted (top) TOMS ozone anomalies and (bottom) MSU temperature anomalies over 1979-1994. QBO effects have been removed, and anomalies are calculated with respect to a 1987-1990 mean of zero. E and P denote the volcanic eruptions of El Chichon and Pinatubo, respectively.

depletion occurs in May-July 1993 (Figure 15), when losses in excess of 4% span the entire NH (Figure 7).

As discussed and referenced above, the following sources of interannual variability in column ozone have been documented using TOMS data: (1) trends (1987-1990 to 1991-1994): 2% (NH) and 2-4% (SH), (2) solar cycle: 2% solar maximum-solar minimum, (3) ENSO: $\pm 1\%$, (4) QBO: $\pm 2-4\%$, and (5) "natural" variability: one-sigma variations of 2% (midlatitudes) and 1% (tropics). The local ozone anomalies observed following Mount Pinatubo are 5-10% (Figure 7), substantially larger than any of these other forced or natural variations. Because of their proximity to Pinatubo and the reasonable agreement with various model calculations (see below), it is fairly certain that a major component of the large ozone losses during these years are attributable to the influence of the Pinatubo volcanic aerosols.

The large ozone losses observed in the NH during winter-spring are likely related to heterogeneous chemical reactions associated with sulfate aerosols [Hofmann and Solomon, 1989; Brasseur and Granier, 1992; Pitari and Rizi, 1993; Rodriguez et al., 1994; Tie et al., 1994; Kinnison et al., 1994]. Manney et al. [1994] have concluded that the 1992-1993 Arctic polar vortex ozone losses were caused by chemical processes. Tie et al. [1994] have calculated a latitude-time variation of column ozone losses over the NH quite similar to that shown in Figure 7. Further calculations with their model suggests that the larger aerial extent of ozone losses during the 1992-93 NH winter results

at least partially from colder temperatures observed during that winter (see Figure 13) (X. X. Tie, personal communication, 1994)). These aerosol-associated ozone loss mechanisms over midlatitudes (outside of the polar vortex) also agree with the detailed calculations of Norton and Chipperfield [1995], who show relatively little transport of polar stratospheric cloud (PSC) processed air across the vortex boundary to midlatitudes during the 1992-1993 winter.

The vertical structure of ozone depletion has been studied here by comparing HALOE and MLS profile measurements between the years 1992-1994, for time periods of near-normal versus large column ozone depletions. Interannual differences in vertical structure are very similar between the HALOE and MLS data. These data (Figure 9) show NH midlatitude ozone depletions during winter 1993 (compared to 1992 and 1994) of 5-10% over 22-35 km, and larger losses (20-30%) at lower altitudes (17-22 km). These latter values agree well with the pre- versus post-Pinatubo ozonesonde comparisons shown by Kerr et al. [1993] and Hofmann et al. [1994a]. Ozone losses in the SH subtropics in 1992 are 5-10% over 22-35 km (Figure 12) but do not extend to lower altitudes. Furthermore, a clear ozone increase of 3-10% is observed over 40-55 km at this time in both HALOE and MLS data. Our analyses of the SBUV/2 profile information did not reveal systematic anomaly structures similar to the column ozone data (the anomalies were more noiselike), but this is not surprising given the low vertical resolution of SBUV/2 (of order 10 km), and the lack of profile information below 25 km [Rodgers, 1990].

There is a strong positive correlation between month-to-month "natural" variations of column ozone and lower stratospheric temperature over high latitudes of both hemispheres [Newman and Randel, 1988; Wirth, 1993; Randel and Cobb, 1994]. This coupling for monthly timescale variations is mainly dynamical in origin, reflecting the similarly signed background gradients of ozone and potential temperature; radiative coupling effects become more important for anomalies with longer timescales (comparable to the radiative relaxation timescale in the lower stratosphere, of order 50-100 days). Comparison of Figures 7 and 13b show such positively correlated ozone-temperature anomalies in the high-latitude SH; note particularly the persistent low temperatures found in association with the Antarctic ozone hole in 1993. Such low temperatures in winter and early spring may help cause the deepened ozone hole (via low-temperature chemical effects [Hofmann et al., 1994b]), whereas the persistence of the cold temperatures through December may be a result (radiatively) of the depleted ozone [Shine, 1986; Kiehl et al., 1988; Ramaswamy et al., 1992; Mahlman et al., 1994]. Similarly, the anomalously cold NH summer polar stratosphere during 1993 (Figure 14) is likely a radiative effect of the depleted ozone during 1993.

Similar ozone-temperature anomaly correlations are not evident in the NH in Figures 7 and 13b, probably because they are obscured by the large, persistent ozone losses. However, one might use the observed temperature anomalies (Figure 13b) to qualitatively assess the dynamical component of ozone variation in the high latitude NH (i.e., it should be similarly signed to the temperature anomalies). This would suggest that positive "dynamical" ozone anomalies were present during January-March 1992, that is, that the "chemical" anomalies were somewhat larger than those shown in Figure 7. This reasoning also suggests that part of the large negative ozone anomalies in early winter 1993 are dynamical in origin, although the timescale of the temperature anomalies is so long (> 4 months) that the temperature is likely

responding radiatively in spring and summer to the depleted ozone levels. It should be emphasized that these dynamical (short time scale) ozone variations are only qualitatively discussed here; the dynamical, radiative, and chemical processes associated with ozone variability are sufficiently tied together so that linear separation is not possible.

Acknowledgments. We thank the TOMS group at Goddard Space Flight Center for on-line access to Meteor 3 TOMS data, and Jim Gleason of NASA for several insightful discussions. John Gille and Dan Packman provided the mapping routine used on the SBUV/2 data. Dorothy Quincy at the Climate Modeling and Diagnostics Laboratory in Boulder, and Ed Hare of the Canadian Atmospheric Environmental Service, supplied the Dobson column ozone data. John Christy (Huntsville) and Jim Hurrell (NCAR) helped with acquisition of the MSU temperature data. Barbara Naujokat supplied recent QBO winds. Access to HALOE and MLS data were provided by the UARS collaborative research at NCAR under John Gille. Xue Xi Ti and Michael Coffey provided careful reviews and insightful discussions. Marilena Stone expertly prepared the manuscript. This work was supported under NASA grants W-16215 and W-18181, and NOAA grant NAAZ0000300149. NCAR is sponsored by the National Science Foundation.

References

Angell, J. K., Comparison of stratospheric warming following Agung, El Chichon and Pinatubo volcanic eruptions, *Geophys. Res. Lett.*, **20**, 715-718, 1993.

Bhartia, P. K., J. Herman, R. D. McPeters, and O. Torres, Effect of Mount Pinatubo aerosols on total ozone measurements from backscatter ultraviolet (BUV) experiments, *J. Geophys. Res.*, **98**, 18,547-18,555, 1993.

Bluth, G.J.S., S. D. Doiron, C. C. Schnetzler, A. J. Kreuger, and L. S. Walter, Global tracking of the SO₂ clouds from the June 1991 Mount Pinatubo eruptions, *Geophys. Res. Lett.*, **19**, 151-154, 1992.

Bojkov, R. D., C. S. Zerefos, D. S. Balis, I. C. Ziomas, and A. F. Bais, Record low total ozone during northern winters of 1992 and 1993, *Geophys. Res. Lett.*, **20**, 1351-1354, 1993.

Bowman, K. P., Global patterns of the quasi-biennial oscillation in total ozone, *J. Atmos. Sci.*, **46**, 3328-3343, 1989.

Brasseur, G., and C. Granier, Mount Pinatubo aerosols, chlorofluorocarbons and ozone depletion, *Science*, **257**, 1239-1242, 1992.

Chandra, S. and R. S. Stolarski, Recent trends in stratospheric total ozone: Implications of dynamical and El Chichon perturbations, *Geophys. Res. Lett.*, **18**, 2277-2280, 1991.

Chandra, S., Changes in stratospheric ozone and temperature due to the eruptions of Mt. Pinatubo, *Geophys. Res. Lett.*, **20**, 33-36, 1993.

Froidevaux, L., J. W. Waters, W. G. Read, L. S. Elson, D. A. Flower, and R. F. Jarnot, Global ozone observations from UARS MLS: An overview of zonal mean results, *J. Atmos. Sci.*, **51**, 2846-2866, 1994.

Gleason, J. F., et al., Record low global ozone in 1992, *Science*, **260**, 523-526, 1993.

Grant, W. B., et al., Aerosol-associated changes in tropical stratospheric ozone following the eruption of Mount Pinatubo, *J. Geophys. Res.*, **99**, 8197-8211, 1994.

Herman, J. R., and D. Larko, Low ozone amounts during 1992-1993 from Nimbus 7 and Meteor 3 total ozone mapping spectrometers, *J. Geophys. Res.*, **99**, 3483-3496, 1994.

Herman, J. R., et al., Meteor 3/total ozone mapping spectrometer observations of the 1993 ozone hole, *J. Geophys. Res.*, **100**, 2973-2983, 1995.

Hofmann, D. J., and S. Solomon, Ozone destruction through heterogeneous chemistry following the eruption of El Chichon, *J. Geophys. Res.*, **94**, 5029-5041, 1989.

Hofmann, D. J., S. J. Oltmans, W. D. Komhyr, J. M. Harris, J. A. Lathrop, A. O. Langford, T. Deshler, B. J. Johnson, A. Torres, and W. A. Mathews, Ozone loss in the lower stratosphere over the United States in 1992-1993: Evidence for heterogeneous chemistry on the Pinatubo aerosol, *Geophys. Res. Lett.*, **21**, 65-68, 1994a.

Hofmann, D. J., S. J. Oltmans, J. A. Lathrop, J. M. Harris, and H. Vömel, Record low ozone at the South Pole in the spring of 1993, *Geophys. Res. Lett.*, **21**, 421-424, 1994b.

Hood, L. L., and J. P. McCormack, Components of interannual ozone change based on Nimbus 7 TOMS data, *Geophys. Res. Lett.*, **19**, 2309-2312, 1992.

Kerr, J. B., D. I. Wardle, and D. W. Tarasick, Record low ozone values over Canada in early 1993, *Geophys. Res. Lett.*, **20**, 1979-1982, 1993.

Kiehl, J. T., B. A. Boville, and B. P. Briegleb, Response of a general circulation model to a prescribed Antarctic ozone hole, *Nature*, **332**, 501-504, 1988.

Kinne, S., O. B. Toon, and M. J. Prather, Buffering of stratospheric circulation by changing amounts of tropical ozone: A Pinatubo case study, *Geophys. Res. Lett.*, **19**, 1927-1930, 1992.

Kinnison, D. E., K. E. Grant, P. S. Connell, D. A. Rotman, and D. J. Wuebbles, The chemical and radiative effects of the Mount Pinatubo eruption, *J. Geophys.*, **99**, 25,705-25,731, 1994.

Komhyr, W. D., R. D. Grass, R. D. Evans, R. K. Leonard, D. M. Quincy, D. J. Hofmann, and G. L. Koenig, Unprecedented 1993 ozone decrease over the United States from Dobson spectrophotometer observations, *Geophys. Res. Lett.*, **21**, 201-204, 1994.

Labitzke, K., and M. P. McCormick, Stratospheric temperature increases due to Pinatubo aerosols, *Geophys. Res. Lett.*, **19**, 207-210, 1992.

Mahlman, J. D., J. P. Pinto, and L. J. Unsheid, Transport, radiative and dynamical effects of the Antarctic ozone hole: A GFDL 'SKYHI' model experiment, *J. Atmos. Sci.*, **51**, 489-508, 1994.

Manney, G. L., et al., Chemical depletion of ozone in the Arctic lower stratosphere during winter 1992-93, *Nature*, **370**, 429-434, 1994.

McCormick, M. P., and R. E. Viegas, SAGE II measurements of early Pinatubo aerosols, *Geophys. Res. Lett.*, **19**, 155-158, 1992.

Newman, P. A., and W. J. Randel, Coherent ozone-dynamical changes in the southern hemisphere spring, 1979-1986, *J. Geophys. Res.*, **93**, 12,585-12,606, 1988.

Norton, W. A., and M. P. Chipperfield, Quantification of the transport of chemically activated air from the northern hemisphere polar vortex, *J. Geophys. Res.*, in press, 1995.

Pitari, G., and V. Rizi, An estimate of the chemical and radiative perturbation of stratospheric ozone following the eruption of Mt. Pinatubo, *J. Atmos. Sci.*, **50**, 3260-3276, 1993.

Planet, W. G., J. H. Lienesch, A. J. Miller, R. Nagatani, R. D. McPeters, E. Hilsenrath, R. P. Cebula, M. T. DeLand, C. G. Wellemeyer, and K. Horvath, Northern hemisphere total ozone values from 1989-1993 determined with the NOAA-11 Solar Backscatter Ultraviolet (SBUV/2) instrument, *Geophys. Res. Lett.*, **21**, 205-208, 1994.

Ramaswamy, V., D. Schwarzkopf, and K. P. Shine, Radiative forcing of climate from halocarbon-induced global stratospheric ozone loss, *Nature*, **355**, 810-812, 1992.

Randel, W. J., and J. B. Cobb, Coherent variations of monthly mean total ozone and lower stratospheric temperature, *J. Geophys. Res.*, **99**, 5433-5447, 1994.

Rodgers, C. D., Characterization and error analysis of profiles retrieved from remote sounding measurements, *J. Geophys. Res.*, **95**, 5587-5595, 1990.

Rodriguez, J. M., M.K.W. Ko, N. D. Sze, C. W. Heisey, G. K. Yue, and M. P. McCormick, Ozone response to enhanced heterogeneous processing after the eruption of Mt. Pinatubo, *Geophys. Res. Lett.*, **21**, 209-212, 1994.

Russell, J. M. III, L. L. Gordley, J. H. Park, S. R. Drayson, W. D. Hesketh, R. J. Cicerone, A. F. Tuck, J. E. Frederick, J. E. Harries, and P. J. Crutzen, The halogen occultation experiment, *J. Geophys. Res.*, **98**, 10,777-10,797, 1993.

Schoeberl, M. R., P. K. Bhartia, E. Hilsenrath, and O. Torres, Tropical ozone loss following the eruption of Mt. Pinatubo, *Geophys. Res. Lett.*, **20**, 29-32, 1993.

Shine, K. P., On the modeled thermal response of the Antarctic stratosphere to a depletion of ozone, *Geophys. Res. Lett.*, **13**, 1331-1334, 1986.

Shiotani, M., Annual quasi-biennial and El Nino-Southern Oscillation (ENSO) timescale variations in equatorial total ozone, *J. Geophys. Res.*, **97**, 7625-7633, 1992.

Spencer, R. W., and J. R. Christy, Precision lower stratospheric monitoring with the MSU: Technique, validation and results 1979-1991, *J. Clim.*, **6**, 1194-1204, 1993.

Stolarski, R. S., P. Bloomfield, R. D. McPeters, and J. R. Herman, Total ozone trends deduced from Nimbus 7 TOMS data, *Geophys. Res. Lett.*, **18**, 1015-1018, 1991.

Tie, X. X., G. P. Brasseur, B. Briegleb, and C. Granier, Two-dimensional simulation of Pinatubo aerosol and its effect on stratospheric ozone, *J. Geophys. Res.*, **99**, 20,545-20,562, 1994.

- Trepte, C. R., R. E. Viegas, and M. P. McCormick, The poleward dispersal of the Mount Pinatubo volcanic aerosol, *J. Geophys. Res.*, **98**, 18,563-18,573, 1993.
- Wallace, J. M., R. L. Panetta, and J. Estberg, Representation of the equatorial stratospheric quasi-biennial oscillation in EOF phase space, *J. Atmos. Sci.*, **50**, 1751-1762, 1993.
- Wirth, V., Quasi-stationary planetary waves in total ozone and their correlation with lower stratospheric temperature, *J. Geophys. Res.*, **98**, 8873-8882, 1993.
- World Meteorological Organization (WMO), Scientific assessment of ozone depletion: 1994, *Rep. 37*, World Meteorol. Org. Global Ozone Res. and Monit. Proj., Geneva, 1995.
- Yang, H., and K. K. Tung, Statistical significance and pattern of extratropical QBO in column ozone, *Geophys. Res. Lett.*, **21**, 2235-2238, 1994.
- Young, R. E., H. Houben, and O. B. Toon, Radiatively forced dispersion of the Mt. Pinatubo volcanic cloud and induced temperature perturbations in the stratosphere during the first few months following the eruption, *Geophys. Res. Lett.*, **21**, 369-372, 1994.
- Zerefos, C. S., K. Tourpali, and A. F. Bais, Further studies on possible volcanic signal to the ozone layer, *J. Geophys. Res.*, **99**, 25741-25746, 1994.
-
- L. Froidevaux and J. W. Waters, Jet Propulsion Laboratory, California Institute of Technology, Pasadena, CA 91109.
- W. J. Randel and F. Wu, National Center for Atmospheric Research, P. O. Box 3000, Boulder, CO 80307. (e-mail: randel@ncar.ucar.edu)
- J. M. Russell III, NASA Langley Research Center, Hampton, VA 23665.

(Received October 31, 1994; accepted March 9, 1995.)